Available online at www.sciencedirect.com

ScienceDirect

Energy Procedia 158 (2019) 1737–1743

Energy Procedia

www.elsevier.com/locate/procedia

10th International Conference on Applied Energy (ICAE2018), 22-25 August 2018, Hong Kong, China

Performance prediction of a reciprocating piston expander with semi-empirical models

Bianchi M., Branchini L., De Pascale A.*, Melino F., Ottaviano S., Peretto A., Torricelli N.

Università di Bologna – DIN, Viale del Risorgimento 2, 40136, Bologna, Italy

Abstract

The aim of this study is to characterize a prototype of reciprocating piston expander integrated into a micro-ORC system test bench (in the kW range of power), installed at the laboratory of the university of Bologna. In order to simulate behavior and performances of the expander in not yet explored operating conditions, two semi-empirical models proposed in the literature have been opportunely adapted to the case of study and calibrated over a full set of available experimental data. One model is based on polynomial correlations on the expander efficiencies, whereas the other one is based on a lumped parameters approach with a more physical sense. Both the models have been evaluated on the error on predict the outputs and compared into performance prediction maps. The preliminary results demonstrate that the polynomial fitting functions model is the most accurate in predicting the outputs in the range of the explored working conditions. However, in order to verify the models extrapolation capability, more experimental points should be collected. The validation of the models outside the calibration range will be object of further investigations.

Keywords: ORC; reciprocating piston expander; modelling; semi-empirical model

1. Introduction

The mathematical models existing for reciprocating piston expanders are, with only few exceptions, deterministic or geometrical models, meaning that a detail description of the geometry of the expander is required in order to compute the state of the fluid inside the machine. Usually, as regards prototypal expanders, complete information about the internal geometry are not available and are known solely to the manufacturer itself, therefore it could be necessary to implement a model with a semi-empirical approach.

10.1016/j.egypro.2019.01.403

Nomenclature		*Subscripts*	
h	Enthalpy [kJ/kg·K]	*amb*	Ambient
$\dot{m}$	Mass flow rate [kg/s]	*0*	Clearance
N	Rotational speed [rpm]	*exp*	Expansion
p	Pressure [Pa]	*comp*	Compression
$\dot{W}$	Power [W]	*sh*	Shaft
Q	Heat flow [W]	*gen*	Generator
T	Temperature [K]	*su*	Supply
V	Volume [m^3]	*ex*	Exhaust
A	Area [m^2]	*el*	Electric
r_v	Volumetric ratio [-]	*leak*	Leakage
AU	Overall heat transfer coefficient [W/K]	*loss*	Losses
N_{test}	Number of test points [-]	*calc*	Calculated
MRE	Mean relative error [-]	*meas*	Measured
		is	Isoentropic
Greek letters		*v*	Volumetric
Δ	Difference [-]	*ref*	Reference
η	Efficiency [-]	*wall*	Wall
ρ	Density [kg/m^3]	*cond*	condenser

Semi-empirical models relies on a limited number of physically meaningful equations and on some essential empirical parameters that must be calibrated with experimental data. Semi-empirical models have been extensively used for the sizing and the performance prediction of compressors, expanders and pumps components of Organic Rankine Cycles (ORC). Many modelling studies in the open literature deserved attention to the simulation of scroll [1-3] and screw expanders [4] for low to medium power output ORC applications, and a rotatory vane expander has been investigated too [5]. Whilst, the open literature on reciprocating piston expanders is very limited: a steady-state simulation model is proposed by Glavatskaya et al. [6]. It has been validated and the performance study of the expansion machine is also carried out. Moreover, a detailed analysis of the extrapolation performance of this semi-empirical model is conducted by Dumont et al. [7].

This paper compares the result of the application of different semi-empirical models, proposed in the open literature, for simulating a reciprocating piston expander prototype, integrated in a micro-ORC system test bench at the University of Bologna, developed in the around-kW range of power. This paper focuses on the modelling of the reciprocating piston expander. More information about the micro-ORC system and its components can be found in the dedicated papers [9,10], where a complete overview has been presented. The models selected for this study are two: the first one is based on the lumped parameters approach proposed by Glavatskaya et al. [6], whereas the second one, proposed by Li [8], uses polynomial functions to fit in volumetric and isoentropic efficiency of the expander, for the characterization of volumetric compressors. Both the models have been adapted to the case of study and calibrated on the same set of experimental data. Finally, the models have been evaluated on the error obtained on prediction of the model outputs and they have been compared into performance prediction maps.

2. Expander models

2.1. Polynomial fitting functions model

In their work, Li [8] presented a simplified model for volumetric compressors based on the definition of the volumetric and isoentropic efficiencies. A similar approach can be applied to expander machines with limited changes to the original equations. The isoentropic efficiency and the volumetric efficiency can be defined by Equation (1) and Equation (2), and are interpolated by the following fitting polynomials as function of the expansion pressure ratio (Equation (3) and Equation (4), respectively).

$$\eta_{is} = \frac{\dot{W}_{el}}{\dot{m} \cdot (h_{su} - h_{ex,is})} \quad (1), \qquad \eta_v = \frac{m_{in} 60}{N V_s \rho_{su}} \quad (2), \qquad \eta_{is} = a_2 \left(\frac{p_{su}}{p_{ex}}\right)^2 + a_1 \left(\frac{p_{su}}{p_{ex}}\right) + a_0 \quad (3), \qquad \eta_v = b_2 \left(\frac{p_{su}}{p_{ex}}\right)^2 + b_1 \left(\frac{p_{su}}{p_{ex}}\right) + b_0 \quad (4)$$

The model takes into account the leakage losses, the friction losses, the heat losses to the ambient and the losses due to the electro-mechanical conversion at the generator. As shown in Figure 1, the model is developed around an isentropic expansion process that elaborates the mass flow rate, $\dot{m}_{in}$, and produces the power output $\dot{W}_{int}$. The mass flow rate actually elaborated by the expander, $\dot{m}_{in}$, corresponds to the difference between the supply mass flow rate, $\dot{m}_{su}$, and the one that by-passes the internal expansion process, $\dot{m}_{leak}$, representing the leakages and indicated by the green line. Internal leakages are taken into account into the volumetric efficiency term. The shaft power, $\dot{W}_{sh}$, is defined on the difference between the internal power, $\dot{W}_{int}$, and the friction losses, $\dot{W}_{loss}$. The isoentropic efficiency is used to compute the shaft power and takes in account the friction losses. The mechanical losses are considered equal to the heat transfer losses. The latter are computed by using an overall heat transfer coefficient that depends on the Nusselt number through an empirical correlation. Finally, the electric power, $\dot{W}_{el}$, is calculated as the product between the shaft power and the mechanical-to-electric power conversion efficiency.

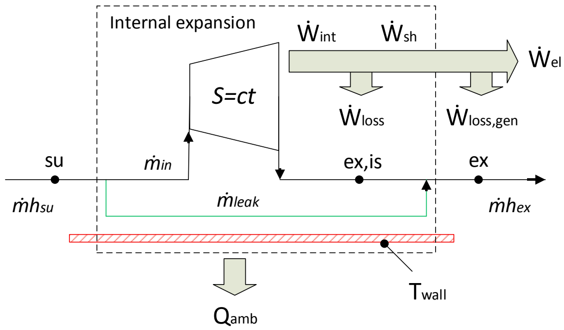

Figure 1. polynomial fitting functions model scheme.

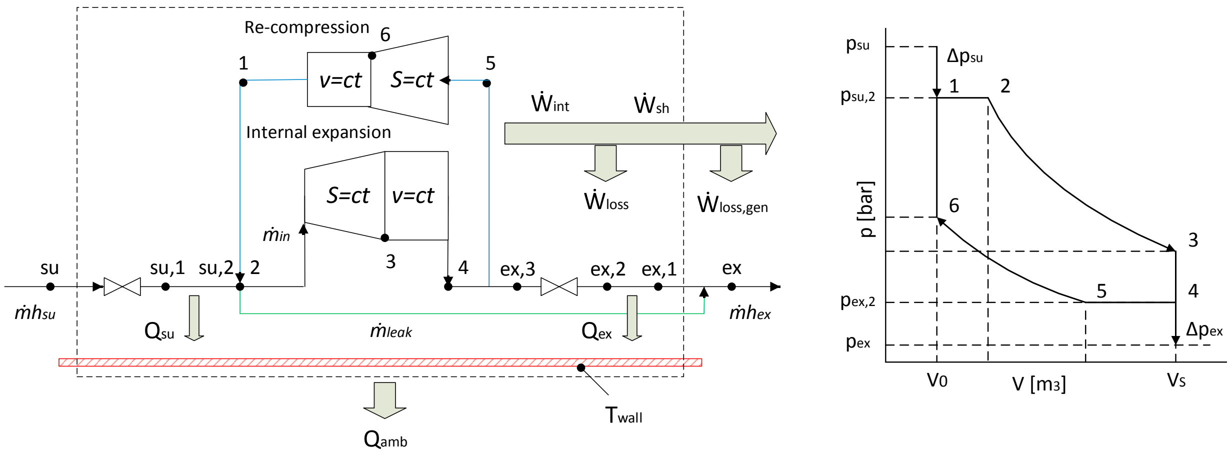

Figure 2. Lumped parameters model scheme and the respective PV diagram representing the internal expansion process.

2.2. Lumped parameters model

The model proposed by Glavatskaya et al. [6] can account different sources of losses that affect the power generated by the expander and the mass flow rate it displaces. These sources are pressure drops across the valves, heat transfers, leakages, re-compression losses and mechanical losses.

The model assumes that the path of the fluid across the expander, from the supply valve to the discharge one, is divided in consecutive steps (as depicted in Figure 2): (su-su$_1$) adiabatic supply pressure drop through the supply valve; (su$_1$-su$_2$) supply cooling down due to the heat exchange between the fluid and the wall; (su$_2$-ex) leakage mass flow rate that by-pass the internal expansion; (2-3-4) internal expansion process in two stages: (2–3) isoentropic and (3–4) at constant volume; (5-6-1) partial re-compression of the residual mass of fluid trapped into the clearance volume, in two stages: (5–6) isoentropic and (6–1) at constant volume; (ex$_3$–ex$_2$) adiabatic discharge pressure drop through the discharge valve discharge; (ex$_2$–ex$_1$) heating up due to the heat exchange between the wall and the fluid. The internal expansion process is composed by the steps 1-6 described by the indicator theoretical diagram presented in Figure 2. Pressure drops are modelled as isoentropic flows through convergent nozzles, whose section A_{su} and A_{ex} are parameters to identify. The heat transfers are computed by means of nominal heat transfer coefficients, $AU_{su,ref}$, $AU_{ex,ref}$ and AU_{amb}. The leakage mass flow rate is also modelled like an isoentropic flow through a convergent nozzle, with a throat section area, A_{leak}. Mechanical losses are determined by the sum of a constant term $W_{loss,ref}$ and a loss proportional to the rotational speed though the parameter $W_{loss,N}$. Re-compression phenomena are modelled by means of a two stage compression of the fluid trapped in the clearance volume V_0.

3. Experimental data

Both the models have been calibrated over the experimental points collected during an extended experimental campaign. The volumetric machine has been tested over 30 working points, characterized by different values of mass flow rate, supply temperature and pressure ratio. The ranges of the explored operating conditions are reported in Table 1, where it is indicated what are the imposed variables and the quantities measured during test.

Table 1. Test conditions.

Experimental set points				Experimental outputs			
$\dot{m}$ [kg/s]	T_{su} [°C]	ΔT_{su} [°C]	p_{ex} [bar]	p_{su} [bar]	T_{ex} [°C]	N [rpm]	P_{el} [W]
0.05-0.14	64.3-86	10.5-40.5	5.7-8.4	10.7-16.9	39.4-72.3	319-963	250-1120

4. Calibration of the model parameters

Both models implemented need, as input variables, the supply temperature, the supply pressure, the exhaust pressure, the ambient temperature and the mass flow rate. The swept volume is known and equal to 230 cm^3, like the nominal generator efficiency, equal to 90 %. Once the parameters are calibrated, the models can predict the values of the exhaust temperature, of the shaft rotational speed and of the electrical power.

The aim of the calibration process is to identify the parameters of the model that optimize the agreement between the calculated outputs and the measured data. The fitting coefficients for the isentropic efficiency, a_i, and for the volumetric efficiency, b_i, of the polynomial fitting functions model, are determined by simply fitting the available experimental data with second degree polynomial functions, using the "polyfit" function available on MATLAB environment. The CoolProp library is used to compute the refrigerant proprieties.

The parameters of the lumped parameters model are identified by minimizing a global error function (Equation (5)) accounting of the errors on prediction of the outputs: the exhaust temperature, the rotational speed and the electric power produced. The minimization process is performed by implementing the model and employing the genetic algorithm routine available in the MATLAB Optimization Toolbox.

$$f = \frac{1}{3}\sqrt{\frac{1}{N_{test}}\sum_{i=1}^{N_{test}}\left(\frac{T_{ex,calc,i}-T_{ex,meas,i}}{T_{ex,calc,i}}\right)^2} + \frac{1}{3}\sqrt{\frac{1}{N_{test}}\sum_{i=1}^{N_{test}}\left(\frac{N_{calc,i}-N_{meas,i}}{N_{calc,i}}\right)^2} + \frac{1}{3}\sqrt{\frac{1}{N_{test}}\sum_{i=1}^{N_{test}}\left(\frac{P_{el,calc,i}-P_{el,meas,i}}{P_{el,calc,i}}\right)^2} \quad (5)$$

Table 2. Identified parameters for the polynomial fitting functions model.

a_2	a_1	a_0	b_2	b_1	b_0
-0.2078	0.9380	-0.6149	-0.2906	1.2297	-0.9738

Table 3. Identified parameters for the lumped parameters model.

AUsu,ref [W/K]	AUex,ref [W/K]	AUamb [W/K]	Wloss,ref [W]	Wloss,N [W/rpm]	Aleak [m^2]	Asu [m^2]	r_{vcomp} [-]	r_{vexp} [-]	V_0 [m^3]
0.17	28.5	0.5	0.1	0.47	7.1 e-06	1.6 e-03	1.03	2.09	4.5 e-05

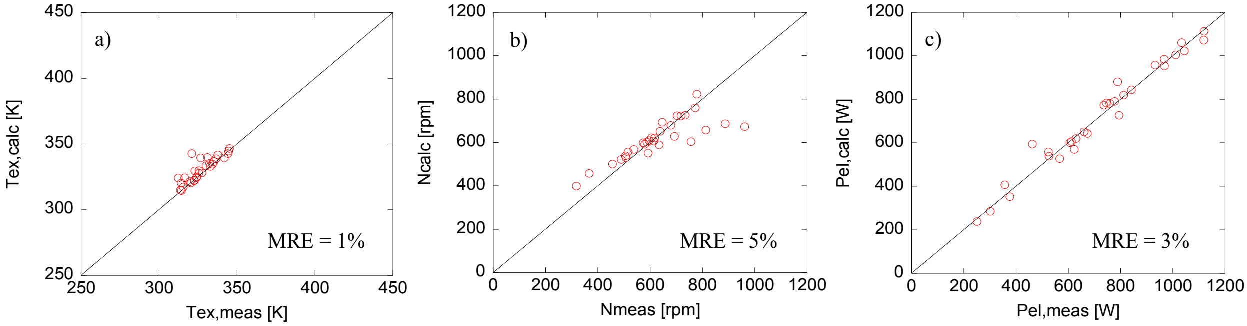

Figure 3. Parity plots obtained by applying polynomial fitting functions model: a) exhaust temperature, b) rotational speed, c) electric power.

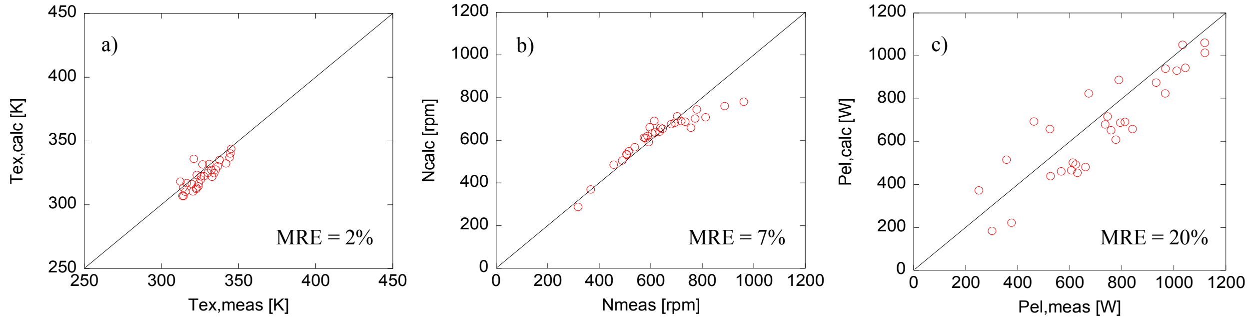

Figure 4. Parity plots obtained by applying lumped parameters model: a) exhaust temperature, b) rotational speed, c) electric power.

5. Results and comparisons

5.1. Results of the calibration process

The coefficients obtained from the calibration process of the polynomial fitting functions model, are presented in Table 2 and the parameters identified by the calibration process of the lumped parameters model are listed in Table 3. Furthermore, a sensitivity analysis of the global error function, while varying the model parameters, has been conducted for the lumped parameters model: the analysis shows that the most influent parameters are r_{vexp} and A_{leak}.

The outputs predicted by the model are compared to the experimental measurements and parity plots are used to display the quality of the fit. Figure 3 shows the simulation results obtained by applying the polynomial fitting functions model, whereas Figure 4 shows the ones obtained by applying the lumped parameters approach. The value of the global error obtained by the minimization process is of 11.2 % for the lumped parameters model and of 2.7 % for the polynomial fitting functions one. The results demonstrate that the polynomial fitting functions model is the most accurate in predict the outputs in the range of the explored working conditions, especially as regards the electric power producible by the expander.

5.2. Results of the extrapolation

The calibrated models can be used for parametric studies of the main output variables by varying the inputs of supply temperature, supply pressure, exhaust pressure and mass flow rate. In this paper the trends of the prediction maps of the rotational speed and of the electric power are presented as function of the mass flow rate, in the range that goes from 0.02 kg/s to 0.2 kg/s (Figure 5a and 5b respectively). The supply temperature is fixed at 85°C and the exhaust pressure is kept constant at 6 bar, corresponding to a condensation temperature of 18°C. We assume an experimental trend line of the supply pressure as function of the mass flow rate (in Figure 5a), obtained by interpolating the available experimental data.

Figure 5 shows that both the models produce similar trends of the electric power and of the rotational speed for the points comprehended in the explored range of the mass flow rate. At the contrary, when the mass flow rate exceeds the explored range the two models diverge.

In order to validate the models outside the calibration range more experimental points should be collected, in addition to the 30 investigated points. However, we expect that the lumped parameters model produce more realistic trends in extrapolation, if compared with the polynomial fitting functions, thanks to the presence of more physical rules.

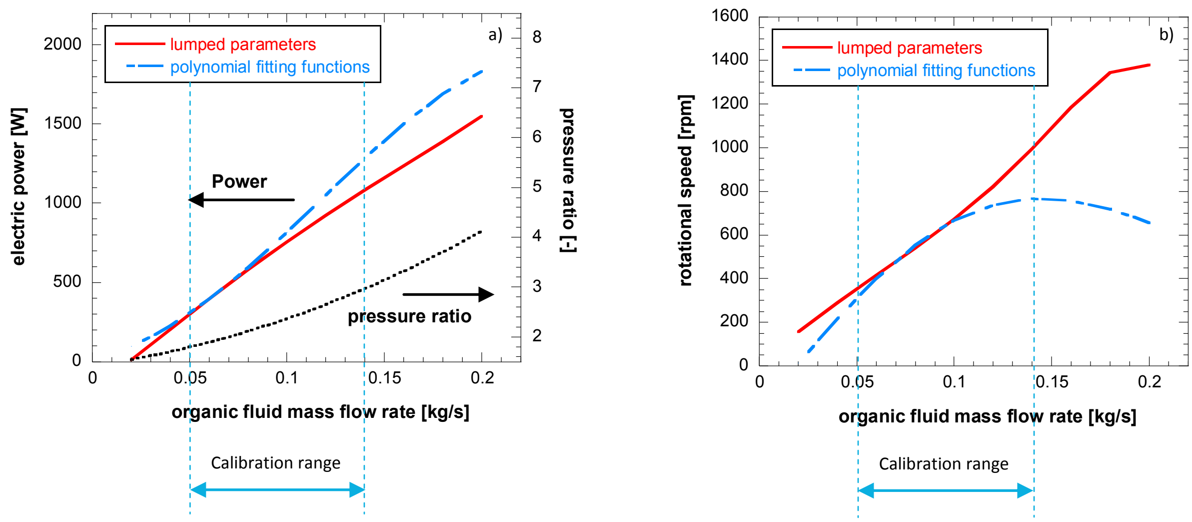

Figure 5. Prediction maps of the rotational speed a) and of the electric power b) as function of the mass flow rate of mass flow rate, at constant conditions of T_{su} = 85°C and p_{ex} = 6bar (T_{cond} = 18bar).

6. Conclusions

This paper presents the results of a preliminary application of two semi-empirical models, adapted an applied to the case of a reciprocating expander. The models have been compared on the error obtained on prediction of the model outputs and they have been used to trace the trends of the electric power and the rotational speed outside the calibration range of mass flow rate.

It results from this study that the polynomial fitting functions model can calculate the outputs in the range of the explored working conditions, with a medium error range of ±2.7 %, whereas the lumped parameters model produces a medium error range of ±11.2 %. Both the models are adapt to describe the behaviour of the expander into the calibration range, but they still need to be validated in extrapolated conditions.

In further studies, we are planning to collect the data necessary for the validation of the models outside the calibration range and perform additional investigations using and adapting the lumped parameter model in different scenarios of this or other expanders with similar architecture.

References

[1] Lemort V., Quoilin S., Cuevas C., Lebrun J. Testing and modelling scroll expander integrated into an organic Rankine cycle. Applied Thermal Engineering 29 (2009) 3094-3102.

[2] Giuffrida A. Modelling the performance of a scroll expander for small organic Rankine cycles when changing the working fluid. Applied Thermal Engineering 70 (2014) 1040-1049.

[3] Ayachi F., Ksayer E.B., Neveu P., Zoughaib A. Experimental investigation and modeling of a hermetic scroll expander. Applied Energy 181 (2016) 256-267.

[4] Ziviani D., Gusev S., Lecompte S., Groll E.A., Braun J.E., Horton W.T., van den Broek M., De Paepe M. Characterizing the performance of a single-screw expander in a small-scale organic Rankine cycle for waste heat recovery. Applied Energy 181 (2016) 155-170.

[5] Vodicka V., Novotny V., Mascuch J., Jolovratnik M. Impact of major leakages on characteristics of a rotatory vane expander for ORC. Energy Procedia 129 (2017) 387-394.

[6] Glavatskaya Y., Podevin P., Lemort V., Shonda O, Descombes G. Reciprocating Expander for an Exhaust Heat Recovery Rankine Cycle for a Passenger Car Application. Energies 5 (2012) 1751-1765.

[7] Dumont O., Dickes R., Lemort V. Extrapolability and limitations of a semi-empirical model for the simulation of volumetric expanders. Energy Procedia 129 (2017) 315-322.

[8] Li W. Simplified steady-state modeling for hermetic compressors with focus on extrapolation. International Journal of Refrigeration 35 (2012) 1722-1733.

[9] Bianchi M., Branchini L., De Pascale A., Orlandini V., Ottaviano S., Pinelli M., Spina P.R., Suman A. Experimental Performance of a Micro-ORC Energy System for Low Grade Heat Recovery. Energy Procedia 129 (2017) 899-906.

[10] Bianchi M., Branchini L., De Pascale A., Orlandini V., Ottaviano S., Peretto A., Melino F., Pinelli M., Spina P.R., Suman A. Experimental Investigation with Steady-State Detection in a Micro-ORC Test Bench. Energy Procedia 126 (201709) 469-476.